



## Original Article

## Proximal Sensor Identification of Lithologic Discontinuities in Eastern Europe

WEINDORF C. David<sup>1\*</sup>, Somsubhra CHAKRABORTY<sup>2</sup>, Laura PAULETTE<sup>3</sup>, Erika MICHÉLI<sup>4</sup>, Bin LI<sup>5</sup>, Titus MAN<sup>6</sup>

<sup>1</sup>Department of Plant and Soil Science, Texas Tech University, Lubbock, TX, USA

<sup>2</sup>Ramakrishna Mission Vivekananda University, Kolkata, India

<sup>3</sup>University of Agricultural Sciences and Veterinary Medicine of Cluj-Napoca, Romania

<sup>4</sup>Szent István University, Gödöllő, Hungary

<sup>5</sup>Louisiana State University, Baton Rouge, LA, USA

<sup>6</sup>Babeş-Bolyai University, Cluj-Napoca, Romania

Received 20 April 2015; received and revised form 15 May 2015; accepted 20 May 2015

Available online 20 June 2015

### Abstract

Lithologic discontinuity identification can be laborious when morphological differences between parent materials are not readily apparent. Often, this requires pedologists to wait for laboratory data that can help differentiate parent materials via physico-chemical properties. In this study, visible near infrared diffuse reflectance spectroscopy (VisNIR DRS) and portable x-ray fluorescence (PXRF) spectrometry, were used to produce quantitative spectral and elemental data supportive of rapid parent material differentiation *in-situ*. Five pedons with suspected lithologic discontinuities were scanned in Hungary and Romania in 2014, morphologically described by trained pedologists, then sampled for standard laboratory characterization. Compared to lab data and/or morphologically described discontinuities, PXRF data was skillful at identifying large, abrupt changes in standardized PXRF differences of elements (DEs), noted in data plots as DE maxima and minima. Standardized VisNIR DRS calculated differences (CDs) in reflectance spectra (350–2500 nm) also identified discontinuities based upon CD reflectance maxima and minima. Within both types of plots, lithologic discontinuities were not well captured by the proximal sensors when CD or DE values fell in active slopes of plot mid-sections. Generally, PXRF appeared slightly better at detecting discontinuities relative to VisNIR DRS. However, VisNIR DRS also showed the ability to identify differences with certain pedons not well captured by PXRF. Both PXRF and VisNIR DRS have been shown to provide useful information which can help in the proper identification of lithologic discontinuities *in-situ*, especially in soils where such features are morphologically nondescript.

**Keywords:** Lithologic discontinuity, pedology, proximal sensors, VisNIR DRS, PXRF.

### 1. Introduction

Lithologic discontinuities (LDs) are defined as a zone within the pedo-stratigraphic column representing a change in lithology or sediment type [23].

Sometimes, LDs are marked by changes in soil texture, coarse fragment content, soil organic carbon, or other physico-chemical parameters. If such features are present, morphological establishment of the LDs is rather simplistic to the trained pedologist. However, many times LDs are less obvious and cannot be easily identified. In fact, many pedologists concede that LDs are frequently not recognized *in-situ* due to a lack of clear morphological expression. Thus,

\* Corresponding author.

Fax: +1806-749-3478

Tel: +1806-742-0775

e-mail: David.weindorf@ttu.edu

pedologists are left to speculate as to the existence of LDs in the field, collect samples, and await the results of physico-chemical laboratory analyses. Lab data typically used for LD establishment include grain size analysis such as ratios of sand/silt, coarse sand/fine gravel fractions, quartz/feldspar ratios, elemental composition, or mineralogy [4, 17, 19, 15, 6]. While effective, such approaches require laboratory analysis and lack field portability/applicability. However, proximal sensors such as portable x-ray fluorescence (PXRF) spectrometry and visible near infrared diffuse reflectance spectroscopy (VisNIR DRS) offer a new means of investigating soil properties *in-situ*, yielding quantitative data on-site. Importantly, these approaches offer advantages over traditional laboratory analyses such as non-destructiveness, alacrity, and low cost.

Portable x-ray fluorescence concerns the use of fluorescent emission spectra produced by elements bombarded with low power x-rays (10-40 kV). The wavelength (energy) of the emitted spectra are unique to each element while the intensity of emissions is proportional to elemental abundance. Conversely, VisNIR DRS involves the use of reflected light in the 350-2,500 nm range. Reflectance spectra are separated into discreet intervals (e.g., 2 to 10 nm) to construct reflectance profiles which are then statistically compared to other quantitative soil data. Various soil parameters are uniquely associated with combinations of specific reflectance spectra [1]. Excellent overviews of PXRF, VisNIR DRS, and their potential synthesis in soil analyses are offered by Weindorf et al. (2014) and Horta et al. (2015), respectively.

Already, VisNIR DRS and PXRF have been independently used to successfully predict a wide range of soil properties, including soil organic carbon [12, 2], gypsum content [30, 34], soil salinity [29], soil pH [21], soil texture [39], soil cation exchange capacity [22], diagnostic subsurface horizons/features [31], soil moisture [38], and organic/inorganic pollutants in soils [35, 1, 32, 14]. Most importantly, Weindorf et al. (2012c) showed that PXRF could be used for enhanced soil horizonation whereby horizons could be differentiated using elemental data from PXRF in nondescript soil profiles. Applied to the present study, VisNIR DRS models have another advantage in that they should be able to better sense irregular decreases in organic carbon

content with depth; an established approach for recognizing buried soils which may or may not also be LDs [10].

Since PXRF and VisNIR DRS have been effective at quantifying numerous soil physico-chemical properties, evaluation of their use for LD establishment seems appropriate. Thus, the objectives of this research were to: 1) morphologically evaluate pedons in Romania and Hungary featuring suspected lithologic discontinuities, 2) scan all pedons with PXRF and VisNIR DRS, 3) subject sampled pedons to standard laboratory characterization, and 4) relate the datasets to determine the effectiveness of PXRF/VisNIR DRS in establishing LD boundaries. We hypothesize that both PXRF and VisNIR DRS will be adept at differentiating parent materials allowing for LD identification. This research presented herein represents a data subset of a larger study by Weindorf et al. (2015).

## 2. Material and Method

### General Occurrence and Features

Five pedons were described, scanned, and sampled in Romania (RO) (n=2), and Hungary (HU) (n=3); the pedons contained a total of 69 samples. Notably, these pedons are part of a larger study with the same foci to include additional pedons from Italy and the United States [37]. The sampling locations were as follows: RO-1 (46.6984 N; 23.5500 E), RO-2 (46.6861 N; 23.5478 E), HU-2 (47.6914 N; 19.6159 E), HU-4 (47.5924 N; 19.3710 E), HU-5 (47.5939 N; 19.3748 E).

Romanian pedons were in Cluj County in the southwest part of the Feleacu Hills at elevations of 708 m (RO-1) and 736 m (RO-2). Geologically, the area is typified by deposits of Miocene age, mostly sands and gravels. The area features an udic moisture regime (663 mm) and mesic temperature regime (8.3°C) [3]. Pedons RO-1 and RO-2 were classified as Fluventic Dystrudepts and Typic Hapludalfs, respectively [25].

Hungarian pedons were developed from pleistocene loess. The composition of the loess for pedon HU-2 (Typic Haplustoll) was influenced by eolian in mixing of more fine material from local sources while pedons HU-4 (Ultic Haplustalf) and HU-5 (Ultic Haplustalf) were more strongly influenced by sand from local sources [25]. Profile HU-2 developed under natural grass vegetation in a table plateau

position. Profiles HU-4 and HU-5 experienced enhanced erosion and translocations of surface materials during the late Pleistocene and the Holocene. The natural vegetation in the Holocene was forest. With annual precipitation approximating is 450-550 mm [27, 11] the moisture regime is ustic and temperature regime is mesic.

Romanian pedons were evaluated in an erosional escarpment and an exposed road cut. Hungarian pedons came from soil pits excavated with a backhoe. At each location, the evaluated area was scraped clean with a knife, then scanned with PXRF at 10 cm increments (e.g., 0-10cm, 10-20 cm, and so on) *in-situ* in a manner consistent with Weindorf et al. (2012c). Field

### Soil Characterization and Proximal Scanning

Upon receipt in the laboratory, all samples were oven dried (40°C) ground to <2 mm, then subjected to standard soil characterization. Particle-size analysis was conducted via hydrometer with clay readings at 1440 min using a model 152-H hydrometer [5]. Sands were wet sieved using a 53 µm sieve, then dried and determined gravimetrically as a percentage of the initial soil weight. Soil reaction (pH) and electrical conductivity (EC<sub>p</sub>) were determined via saturated paste after 24 h equilibration using an Accumet XL20 pH/conductivity meter [18, 24] (Fisher Scientific, Pittsburgh, PA, USA). Soil organic matter (SOM) was determined per Nelson and Sommers (1996) after 8 h of ashing at 400°C to minimize dehydroxilation of mineral soil. Total C total N analysis was conducted via Dumas method high temperature combustion on a LECO TruSpec CN analyzer (St. Joseph, MI) [26]. Detailed methodologies of both VisNIR DRS and PXRF scanning procedures followed as part of this study are given by Weindorf et al. (2015).

### Comparative Discontinuity Indices

In this study, the degree of horizon differentiation within a given pedon was evaluated via principal component analysis (PCA) using the scan layers and the respective soil variables as the data matrix. Essentially, PCA uses an orthogonal transformation to convert a set of observations of possibly correlated variables into a set of values of linearly uncorrelated variables termed principal components, greatly reducing the chance that the correlated variables are repeatedly considered in variance calculations [8]. Thus, the original dataset is projected onto new coordinates

scanning was limited to PXRF only due to logistical limitations related to international transportation of equipment. Following scanning, morphological field evaluation was made per Schoeneberger et al. (2002) with suspected LDs noted at various depths. Field notes were made and profiles were photographed. Soils were sampled at 10 cm increments to align with proximal scanning depths, thus avoiding any bias associated with morphologically established LD boundaries. Samples were sealed in plastic bags and shipped to the Texas Tech University pedology laboratory (Lubbock, TX, USA) for standard characterization. Prior to shipment, samples were dried and crushed in accordance with soil permit import regulations.

samples were oven dried (40°C) ground to <2 mm, then subjected to standard soil characterization. Particle-size analysis was conducted via hydrometer with clay readings at 1440 min using a model 152-H hydrometer [5]. Sands were wet sieved using a 53 µm sieve, then dried and determined gravimetrically as a percentage of the initial soil weight. Soil reaction (pH) and electrical conductivity (EC<sub>p</sub>) were determined via saturated paste after 24 h equilibration using an Accumet XL20 pH/conductivity meter [18, 24] (Fisher Scientific, Pittsburgh, PA, USA). Soil organic matter (SOM) was determined per Nelson and Sommers (1996) after 8 h of ashing at 400°C to minimize dehydroxilation of mineral soil. Total C total N analysis was conducted via Dumas method high temperature combustion on a LECO TruSpec CN analyzer (St. Joseph, MI) [26]. Detailed methodologies of both VisNIR DRS and PXRF scanning procedures followed as part of this study are given by Weindorf et al. (2015).

In this study, pH, EC, sand, silt, clay, and SOM were the lab input variables used for PCA. For each pedon, principal components of laboratory analysis results were extracted in the matrix of correlation with a minimum retained eigen value of 1, maximum iterations of 25, and convergence level of 0.001 [37]. The differences of laboratory analysis (DLAs) between soil layers were established via PCA per Eq. 1:

$$DLA_n = \sqrt{\sum_{i=1}^F (L_{i(n-1)} - L_{in})^2} \quad [1]$$

where,  $DLA_n$  is the difference of laboratory analyses of layer  $n$  to the above layer  $n-1$ ;  $F$  is the total number of significant principal components obtained in PCA;  $L_{i(n-1)}$  and  $L_{in}$  are the PC scores of layer  $n$  and the above layer  $n-1$  on principal component  $i$ , respectively [37].

Since PCA is highly sensitive to the scaling of the variables, the original laboratory analysis results were standardized into the same scale for each pedon as divided by the averages of the variables before the execution of PCA. As the original values of the soil properties were standardized into the same scale and the principal components accounted for 90% of the variances in most cases, the differences between data points in the multidimensional coordinate system of the principal components can therefore be

recognized as the differences of the original dataset [37]. The calculated difference increases with the variation of any soil variable considered.

Portable x-ray fluorescence scanning provides elemental data ~22 elements *in-situ*. Singular or multi-elemental abundance within a given pedon can then be used for horizon differentiation [33]. As such, differences of elements (DEs), as determined by PXRF, between horizons were calculated via Eq. 2:

$$DE_n = \sqrt{\sum_{i=1}^F (L_{i(n-1)} - L_{in})^2}$$

[2]

where,  $DE_n$  is the difference of elemental contents of the layer  $n$  to the above layer  $n-1$  [37]. Similarly, DEs between soil layers increase with the variation of elemental concentrations within the pedon. Fifteen elements, namely K, Ca, Ti, V, Cr, Mn, Fe, Ni, Cu, Zn, Rb, Sr, Zr, Ba, and Pb, were initially selected for PCA in this study. Furthermore, only elements with a measured quantity more than 10 times greater than their reported PXRF errors were selected.

Finally, in the same manner, the calculated differences (CDs) of VisNIR DRS reflectance values between soil layers were established via PCA per Eq. 3 [37]:

$$VisNIRdifferences_n = \sqrt{\sum_{i=1}^F (L_{i(n-1)} - L_{in})^2}$$

[3]

Equations 2 and 3 are essentially the same as Eq. 1, except the PXRF readings of elemental contents and VisNIR DRS reflectance values were used as the matrix for PCA in Eqs. 2 and 3, respectively [37]. Importantly, we only considered a subset (1700-2500nm) of the total VisNIR DRS range shown as the most informative region for SOM [28]. All statistical analyses were executed in XL Stat 2014 (Addinsoft, Paris, France).

### 3. Results and Discussion

#### Field and Lab Assessment

Results of our lab analyses are presented in Table 1. Some analyses of Hungarian samples were not possible due to limited sample quantity available after shipment.

#### Hungary

Hungarian pedons showed differential expression of possible discontinuities. For example, a strong calcic horizon was evident in Pedon HU-2 at 100 cm; a suspected area of discontinuity. However,  $\text{CaCO}_3$  accumulation may also be a product of normal soil development through carbonate translocation and precipitation. The area in question clearly shows a doubling of carbon (1.3 to 2.9%) at the 100 cm boundary. Also, clay content decreases ~4% relative to the overlying horizon. While this decrease is minor, it does cause a textural shift from silty clay loam to silt loam. At 110-120 cm, SOM% reaches a minimum of 0.58%, before steadily increasing below that with depth. This increase in SOM% deep in the profile is quite unusual and gives an indication that a discontinuity in this area may be appropriate as opposed to simple pedogenic calcic horizon development.

Pedon HU-4 showed two possible discontinuities at 90 cm and 146 cm (loess over lacustrine sediments). Both suspected discontinuities were clearly reflected in the lab data. Relative to the overlying horizon, the pH at 90 cm shifts from 4.97 to 7.37, SOM doubles (0.32 to 0.60%), and electrical conductivity triples (107 to 382  $\mu\text{S m}^{-1}$ ).

At 140-150 cm, sand content drops by 22%, silt content increases by 16%, and carbon content increases from 2.35 to 4.07% relative to the overlying horizon. A third suspected discontinuity was also evident in the lab data, though not detected during morphological description. At 110-120 cm, soil texture was silt loam, and carbon was 6.30%, whereas the overlying and underlying horizons were both sandy loam and had carbon contents of 0.34% (above) and 3.89% (below).

Morphological evaluation of Pedon HU-5 suggested a discontinuity at 80 cm. Lab data clearly shows a dramatic shift in physico-chemical properties from 80 to 110 cm. Except for the surface horizon (likely impacted by soil pit spoil), the upper part of the profile is acidic (4.1-4.8) and shows a steady increase in clay content from sandy loam (14% clay), to sandy clay loam (23-31% clay), to clay (40% clay) with depth.

However at 90 cm, clay content decreases, silt content increases, soil pH moderates (and turns alkaline by 100 cm) and carbon levels increase by as much as 20 fold. While the pH and silt content can be linked to calcic horizon formation, this does not explain the decrease in

sand content (68% in the upper part of the profile lowering to 22% by 100 cm). At 80-90 cm, SOM% is also the greatest of any horizon (0.91%) in this profile except for the surface horizon, suggesting a discontinuity in this profile is likely.

### **Romania**

Morphological evaluation of Romanian Pedon RO-1 suggested discontinuities at 21, 78, and 95 cm.

Contrariwise, lab data was largely unremarkable for the first two suspected discontinuities, showing mostly sandy loam and loamy sand textures, and acidic conditions (4.9 to 5.8). However at 95 cm, the texture changes from loamy sand to sandy clay loam, clay content increases from 6 to 23%, carbon content doubles (0.08 to 0.19) and salinity ( $72 \mu\text{S m}^{-1}$ ) is the highest of any horizon except the surface horizon. Since these soils are Fluventic Dystrudepts, clay illuviation in the subsoil is thought to be depositional, lacking any semblance of clay films. Therefore, a discontinuity at this depth is likely.

Pedon RO-2 was suspected of having a discontinuity at 36 cm; an intergrade between mixed colluvium/alluvium transitioning into degrading sandstone. Lab data supporting such a designation chiefly concern textural components. The 40-50 cm depth is a clay loam, surrounded above and below by sandy clay loam.

Similarly, clay content is higher, sand content is lower, and silt content is higher than adjacent horizons. However, the chemical lab data (carbon, nitrogen, pH, salinity) are much less remarkable in their support of a discontinuity at this depth. As such, a discontinuity may be possible at this depth, but is not assured.

### **Proximal Sensor Approaches**

In discussing the ability of PXRf and VisNIR DRS to clearly differentiate profile parent materials, the five evaluated pedons were qualitatively grouped into classes of good, fair, and poor for both VisNIR DRS and PXRf. Notably, these classes were not established strictly by associations with lab-generated data; rather, they were made with consideration of lab data, field morphological description, and consideration of pedogenic processes. In some instances, lab data and/or field suspected discontinuities aligned nicely with PXRf and VisNIR DRS predictive plots. But in other instances, wide discrepancy was

found. Weindorf et al. (2012c; 2014) clearly outlined the rationale for such differences with regard to PXRf as follows: 1) PXRf data aligns well with traditional morphological horizons, 2) PXRf reveals more horizons than traditional morphological descriptions due to differences in elemental concentrations imperceptible to the human eye, or 3) PXRf reveals fewer horizons than morphological descriptions based on differences undetectable to the PXRf (e.g., differences in soil structure, rooting, bulk density, soil organic carbon). Whilst VisNIR DRS should reasonably be able to detect differences in organic carbon [12], other soil characteristics such as bulk density, soil structure, and consistence likely remain undetectable to these two proximal sensors. However, those characteristics seldom form the sole basis for lithologic discontinuity designation.

### **PXRf Assessment**

With regard to PXRf analysis of discontinuity assessment, three pedons qualitatively showed good alignment with lab and/or field established continuities; one pedon was fair, and one was poor. In most instances, PXRf discontinuities were marked by either maximum or minimum DE values evaluated on a pedon by pedon basis (Fig. 1).

In some cases, the maximum and minimum values were helpful in adjusting the depth of the lab/field determined discontinuity where clear trends were observed. All three Hungarian pedons showed good alignment between PXRf and lab/field data [37]. Pedon HU-2 had a field suspected discontinuity at 100 cm. However, lab data suggested that it is more appropriately moved deeper to 110-120 cm. The PXRf DEs reached a maximum at 100 cm and a minimum at ~115 cm, supporting both possibilities. Pedon HU-4 had field suspected discontinuities at 90 and 146 cm.

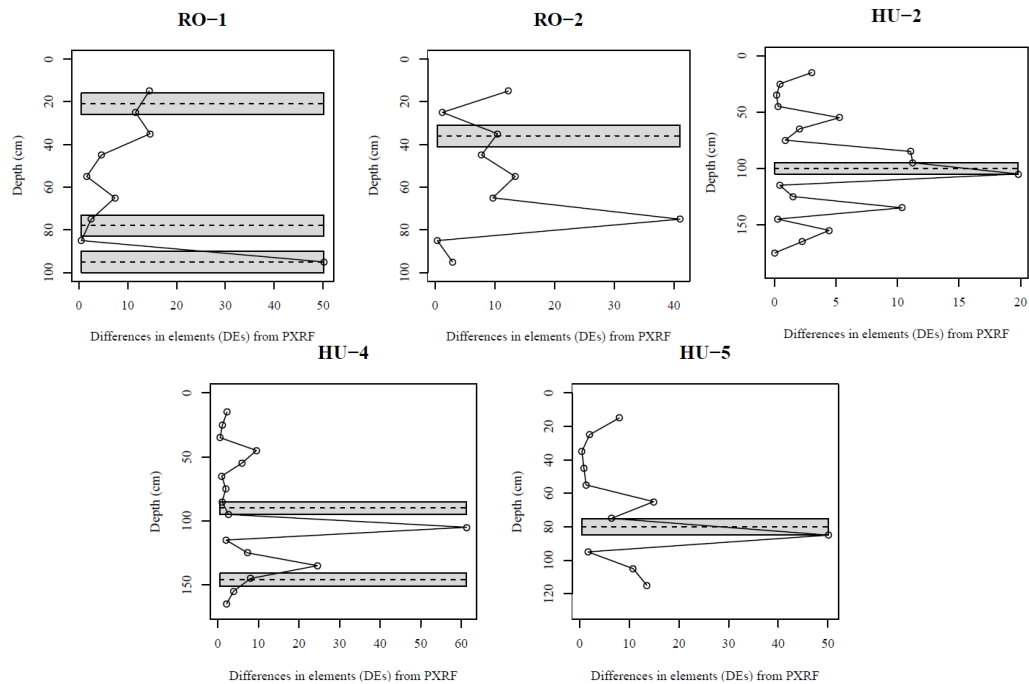
The former was well captured by a PXRf DE minimum, while the latter was not well captured by PXRf; the DE trend line was still decreasing at that depth.

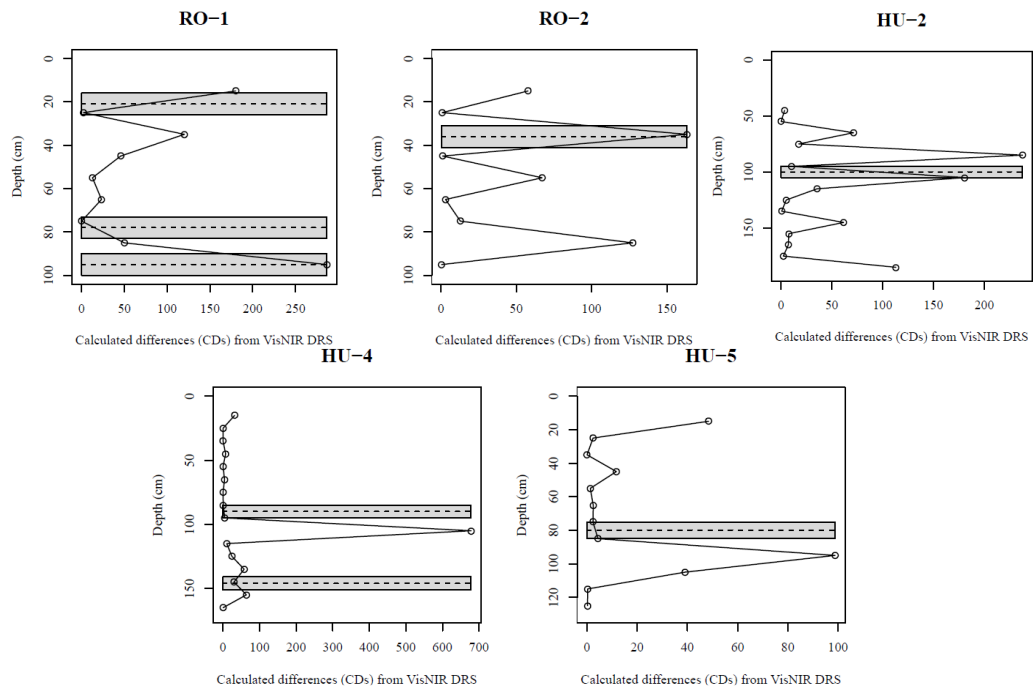
While elusive in the field, lab data shows a possible discontinuity at 110-120 cm; a depth clearly captured by a PXRf DE maximum at ~110 cm. Finally, pedon HU-5 shows a maximum PXRf DE at ~83 cm, clearly reflective of both lab and field discontinuity placement at 80 cm.

Table 1. Soil physicochemical analysis in a lithologic discontinuity study from Hungary and Romania [37]

RO-1										HU-4									
Depth	SOM†	EC‡	pH	Clay	Sand	Silt	Texture§	N	C	Depth	SOM	EC	pH	Clay	Sand	Silt	Texture	N	C
--cm--	---%---	uS m <sup>-1</sup>		-----%				-----%		--cm--	---%---	uS m <sup>-1</sup>		-----%				-----%	
0-10	2.91	67	5.34	8.3	75.2	16.5	SL	0.1132	1.80	0-10	2.55	178	6.45	15.5	64.7	19.8	SL	0.1988	3.47
10-20	1.92	35	5.16	8.3	75.5	16.2	SL	0.0538	1.16	10-20	1.04	481	3.7	17.4	66.5	16.1	SL	0.0811	0.80
20-30	1.29	45	4.90	6.3	76.2	17.6	SL	0.0303	0.58	20-30	0.67	99	4.22	17.4	66.4	16.3	SL	0.0492	0.51
30-40	0.83	20	5.00	6.3	78.0	15.8	LS	0.0217	0.45	30-40	0.71	108	4.31	19.4	64.1	16.5	SL	0.0369	0.42
40-50	0.90	29	4.79	6.3	77.2	16.6	LS	0.0204	0.39	40-50	0.70	99	4.43	21.6	63.7	14.7	SCL	0.0440	0.45
50-60	0.87	20	5.06	6.3	77.6	16.1	LS	0.0099	0.19	50-60	0.70	217	4.41	23.6	61.1	15.3	SCL	0.0479	0.38
60-70	0.75	20	5.55	6.3	78.4	15.4	LS	0.0076	0.11	60-70	0.40	225	4.61	21.7	60.6	17.7	SCL	0.0271	0.25
70-80	0.71	21	5.68	4.2	79.8	15.9	LS	0.0060	0.11	70-80	0.36	110	4.81	15.4	68.9	15.7	SL	0.0306	0.19
80-90	0.72	18	5.79	6.3	79.2	14.5	LS	0.0068	0.09	80-90	0.32	107	4.97	11.3	74.9	13.7	SL	0.0172	0.14
90-100	1.10	72	5.15	22.9	63.5	13.6	SCL	0.0197	0.19	90-100	0.60	382	7.37	15.5	68.9	15.6	SL	0.0268	0.25
<b>RO-2</b>										100-110	0.32	271	7.64	11.2	61.0	27.8	SL	0.0363	0.34
0-10	3.10	70	5.66	10.4	68.4	21.2	SL	0.1371	1.82	110-120	0.11	122	7.89	7.2	37.6	55.2	SiL	0.0284	6.30
10-20	1.43	45	5.52	12.4	69.2	18.5	SL	0.0469	0.60	120-130	0.44	243	8.02	9.3	53.7	37.0	SL	0.0366	3.89
20-30	1.28	89	5.34	16.5	65.9	17.6	SL	0.0389	0.44	130-140	0.24	124	7.94	5.1	85.4	9.5	LS	0.0119	2.35
30-40	1.31	50	5.07	25.1	58.0	17.0	SCL	0.0410	0.30	140-150	0.36	142	8.09	10.3	63.9	25.8	SL	0.0222	4.07
40-50	1.50	63	4.94	34.0	43.9	22.2	CL	0.0340	0.23	150-160	0.07	103	8.00	6.2	87.4	6.4	LS	0.0076	1.74
50-60	1.30	51	4.94	25.2	63.4	11.4	SCL	0.0238	0.14	160-170	0.05	108	8.11	6.2	88.6	5.2	S	0.0150	1.99
60-70	1.15	59	5.02	23.0	69.9	7.1	SCL	0.0298	0.15	<b>HU-5</b>									
70-80	0.59	45	5.05	18.7	78.9	2.5	SL	0.0096	0.07	0-10	3.48	270	7.08	14.5	61.9	23.6	SL	0.3158	3.87
80-90	0.47	49	5.18	14.5	81.0	4.5	SL	0.0165	0.10	10-20	0.86	95	4.21	16.5	66.2	17.3	SL	0.0622	0.74
90-100	0.84	29	5.35	12.4	84.9	2.7	LS	0.0130	0.07	20-30	0.66	94	4.1	14.4	68.4	17.3	SL	0.0528	0.58
<b>HU-2</b>										30-40	0.48	99	4.6	16.4	68.8	14.8	SL	0.0410	0.38
0-10	2.94	391	6.81	--	--	--	--	0.1929	2.21	40-50	0.43	116	4.53	16.5	67.6	15.9	SL	0.0342	0.30
10-20	2.75	327	6.38	--	--	--	--	0.1865	2.08	50-60	0.46	152	4.48	22.8	63.1	14.1	SCL	0.0278	0.25
20-30	2.70	265	5.79	33.4	11.2	55.3	SiCL	0.1809	1.98	60-70	0.65	176	4.85	31.5	48.7	19.8	SCL	0.0297	0.23
30-40	2.50	312	5.74	33.6	10.9	55.6	SiCL	0.1613	1.77	70-80	0.81	262	4.44	40.3	33.2	26.6	C	0.0423	0.24
40-50	2.43	179	5.70	33.6	10.0	56.3	SiCL	0.1592	1.73	80-90	0.91	408	5.79	38.1	29.7	32.2	CL	0.0462	0.32
50-60	--	--	--	--	--	--	--	--	--	90-100	0.48	296	7.69	27.3	22.2	50.5	CL	0.0444	2.77
60-70	1.65	221	6.01	40.0	9.2	50.8	SiC/SiCL	0.0913	1.08	100-110	0.37	277	7.74	16.4	33.3	50.2	SiL	0.0225	6.72
70-80	1.38	378	6.19	35.4	10.5	54.1	SiCL	0.0621	0.77	110-120	0.22	219	7.93	12.4	41.1	46.5	L	0.0177	6.46
80-90	0.90	323	6.45	33.1	11.7	55.1	SiCL	0.0585	0.47	120-130	0.29	239	7.81	12.4	43.8	43.9	L	0.0133	5.81
90-100	0.75	770	7.19	28.9	14.2	56.9	SiCL	0.0518	1.27										
100-110	0.63	873	7.45	24.4	15.3	60.3	SiL	0.0365	2.90										
110-120	0.58	516	7.79	24.5	15.6	60.0	SiL	0.0389	2.73										
120-130	0.81	350	7.61	26.6	15.4	58.0	SiL	0.0450	2.55										
130-140	0.83	344	7.68	28.8	15.4	55.7	SiCL	0.0479	2.32										
140-150	0.91	724	7.70	31.0	15.9	53.1	SiCL	0.0539	2.10										
150-160	1.02	632	7.53	33.0	16.7	50.3	SiCL	0.0584	1.98										
160-170	1.02	1038	7.59	35.3	17.0	47.7	SiCL	0.0604	1.83										
170-180	1.19	964	7.66	37.5	19.8	42.7	SiCL	0.0624	1.66										
180-190	1.04	955	7.66	37.6	24.1	38.4	CL	0.0521	1.16										

†Soil organic matter.  
‡Electrical conductivity.  
§USDA soil textures per Schoeneberger et al. (2002).





**Figure 1.** Differences of element (DEs) and calculated differences (CDs) as determined by portable x-ray fluorescence (PXRF) spectrometry and visible near infrared diffuse reflectance spectroscopy (VisNIR DRS), respectively, for five pedons suspected of having lithologic discontinuities in Romania and Hungary (adapted from Weindorf et al., 2015). Field suspected discontinuity depths are noted with a dashed line bounded by a gray bar of  $\pm 5$  cm.

Romanian pedons RO-1 and RO-2 were considered fair and poor matches to PXRf data, respectively [37]. In RO-1, field suspected discontinuities were noted at 21, 78, and 95 cm.

The first was likely errant, owing to a lack of lab or PXRf data that showed compelling differences relative to overlying or underlying horizons. At 78 cm, PXRf lab data was near the minimum DE, but a slight adjustment to the depth (a few cm deeper) is suggested by the PXRf data.

Then, the suspected 95 cm discontinuity was clearly supported both by lab data as well as a PXRf DE that reached its maximum.

Pedon RO-2 was classed as poor because lab data was inconclusive at the suspected discontinuity depth (36 cm); some shifts in lab data were noted at 40-50 cm but they were meager and PXRf DEs did not support any compelling differences. At 75 cm, a PXRf DE reached its maximum; a possible discontinuity based on lab data.

#### **VisNIR DRS Assessment**

For VisNIR DRS analysis of discontinuity assessment, four pedons qualitatively showed good alignment with lab and/or field established discontinuities; one pedon was fair, and none were poor. Similar to PXRf DE differential, VisNIR DRS identified discontinuities were marked by either maxima or minima in calculated spectral differences (Fig. 1).

Hungarian pedons were generally well described by VisNIR DRS with two pedons showing good and one showing fair alignment with field identified discontinuities [37].

For Pedon HU-2, a field suspected discontinuity at 100 cm is clearly marked by a CD minimum in the VisNIR DRS data. Pedon HU-4 was fair in its assessment, showing a clear CD minimum at one field discontinuity (90 cm), but showing rather unremarkable CD features at the second field discontinuity (146 cm).

Somewhat surprisingly, one of the compelling features of the second discontinuity was a sharp increase in organic carbon, yet VisNIR DRS was unable to capture this in the subsoil pedon CD. Pedon HU-5 showed better alignment with a VisNIR DRS CD minimum aligning well with a field described discontinuity at 80 cm.

Relative to PXRf DEs, VisNIR DRS CDs in the Romanian pedons were comparatively better [37]. In Pedon RO-1, CD minima both aligned nicely with field suspected discontinuities at 21 and 78 cm.

Conversely, in Pedon RO-2, a CD maximum was observed at 36 cm, aligning well with a field described discontinuity at that depth.

#### **Application of VisNIR DRS and PXRf in Discontinuity Evaluation**

While the results of data presented herein indicate that VisNIR DRS is better than PXRf in sensing physico-chemical shifts in evaluated pedons, the full study of 12 pedons by Weindorf et al. (2015) showed that PXRf was slightly better than VisNIR DRS. This suggests that changes in soil mineralogical composition are more efficiently quantified as elemental differences rather than alterations in reflectance spectra. In some pedons, VisNIR DRS can sense differential levels of organic carbon in soils; a parameter imperceptible to PXRf directly. In other instances, PXRf and VisNIR DRS can be used as complimentary approaches to dualistically elucidate differences within a soil profile.

Summarily, we conclude that the data afforded by the use of PXRf and VisNIR DRS offer pedologists unique insight into quantitative differences between soil horizons; differences which may be indicative of lithologic discontinuities. One of the more important conclusions identified by the present study is the concept that relative maxima and minima in either DEs or CDs of PXRf and/or VisNIR DRS data, respectively, can be important indicators of possible changes in soil parent material. Explicitly, we do not advocate the strict use of proximal sensors in the establishment of discontinuities, devoid of lab and morphological data. However, these instruments provide pedologists with ancillary data, quickly and easily acquired *in-situ*, which can help identify areas of lithologic discontinuity within a given pedon, whether visually observable or not. Taken collectively, these proximal sensors can account for shifts in both organic and inorganic soil constituents; changes in which offer insight into the presence of discontinuities.

#### **4. Conclusions**

This research presents partial findings from a study conducted by Weindorf et al. (2015) which evaluated the use of portable x-ray fluorescence (PXRf) spectrometry and visible near infrared diffuse reflectance spectroscopy (VisNIR DRS) for identification of lithologic discontinuities in soils of Romania and Hungary. Five pedons consisting of 69 sampled depths were scanned with both proximal sensors, and the data was then compared to both standard lab-generated soil characterization data as well as morphological descriptive data. Large, abrupt changes in standardized PXRf differences of elements (DEs) often successfully identified discontinuities (whether suggested by lab data and/or morphological description) appearing in the

data plots as DE maxima and minima. Similarly, standardized VisNIR DRS calculated differences (CDs) in reflectance spectra (350-2500 nm) identified discontinuities based upon CD reflectance maxima and minima. With both types of plots, discontinuities were not well captured by the proximal sensors when CD or DE values fell in the mid-section of the plots. Across the five pedons evaluated for this paper, PXRF appeared to show slightly lower detection of discontinuities relative to VisNIR DRS. However, the full study by Weindorf et al. (2015) (12 pedons in all) noted an opposite trend. We recommend the integrated use of proximal sensors in conjunction with lab data and morphological evaluation of lithologic discontinuities in soil profiles especially in instances where differences in parent material are morphologically nondescript.

### Acknowledgements

The authors gratefully acknowledge Taylor Person for her assistance in field sampling and laboratory analysis. The authors gratefully acknowledge financial support of the project from the BL Allen Endowment in Pedology at Texas Tech University.

### REFERENCES

[1] Chakraborty S., D.C. Weindorf, C.L.S. Morgan, Y. Ge, J.M. Galbraith, B. Li, and C.S. Kahlon, 2010, Rapid identification of oil-contaminated soils using visible near-infrared diffuse reflectance spectroscopy. *J. of Env. Qual.* 39:1378-1387. doi:10.2134/jeq2010.0183.

[2] Chakraborty S., D.C. Weindorf, N. Ali, B. Li, Y. Ge, J.L. Darilek, 2013, Spectral data mining for rapid measurement of organic matter in unsieved moist compost. *Appl. Opt.* 52:B82–B92.

[3] Florea N., and I. Munteanu, 2012, The Romanian System of Soil Taxonomy. Sitech, Craiova, Romania.

[4] Foss J.E., and R.H. Rust, 1968, Soil genesis study of a lithologic discontinuity in glacial drift in Western Wisconsin. *Soil Sci. Soc. Am. J.* 32(3):393-398. doi:10.2136/sssaj1968.03615995003200030036x.

[5] Gee G.W., and J.W. Bauder, 1986, Particle-size analysis. p. 383–411. *In* A. Klute (ed.) *Methods of soil analysis*. Part 1. Physical and mineralogical methods. 2nd ed. SSSA, Madison, WI.

[6] Habecker M.A., K. McSweeney, and F.W. Madison, 1990, Identification and genesis of fragipans in Ochrepts of North Central Wisconsin. *Soil Sci. Soc. Am. J.* 54(1):139-146. doi:10.2136/sssaj1990.03615995005400010022x.

[7] Horta A., B. Malone, U. Stockmann, B. Minasny, T.F.A. Bishop, A.B. McBratney, R. Pallasser, and L. Pozza, 2015, Potential of integrated field spectroscopy and spatial analysis for enhanced assessment of soil contamination: A prospective review. *Geoderma* 241-242:180-209. doi:10.1016/j.geoderma.2014.11.024.

[8] Jolliffe, I.T., 1986, *Principal component analysis*. Springer-Verlag, New York.

[9] Kabata-Pendias A., and H. Pendias, 2001, *Trace elements in soils and plants*. CRC Press, Boca Raton, FL.

[10] Kuzila M.S., 1995, Identification of multiple loess units within modern soils of Clay County, Nebraska. *Geoderma* 65:45-57.

[11] Michéli E., M. Fuchs, P. Hegymegi, and P. Stefanovits, 2006, Classification of the major soils of Hungary and their correlation with the World Reference Base for Soil Resources (WRB) – *Agrokémiaés Talajtan* 55(1):19-328.

[12] Morgan C.L.S., T.H. Waiser, D.J. Brown, and C.T. Hallmark, 2009, Simulated in situ characterization of soil organic and inorganic carbon with visible near-infrared diffuse reflectance spectroscopy. *Geoderma* 151(3-4):249-256.

[13] Nelson D.W., and L.E. Sommers, 1996, Total carbon, organic carbon, and organic matter. *In* D.L. Sparks (ed.), *Methods of soil analysis*. Part 3. SSSA Book Ser. 5. SSSA, Madison, WI. p. 961–1010.

[14] Paulette L., T. Man, D.C. Weindorf, and T. Person, 2015, Rapid assessment of soil and contaminant variability via portable x-ray fluorescence spectroscopy: Copşa Mică, Romania. *Geoderma* 243-244:130-140. doi:10.1016/j.geoderma.2014.12.025.

[15] Price T.W., R.L. Blevins, R.I. Barnhisel, and H.H. Bailey, 1975, Lithologic discontinuities in loessial soils of Southwestern Kentucky. *Soil Sci. Soc. Am. J.* 39(1):94-98. doi:10.2136/sssaj1975.03615995003900010026x.

[16] R Development Core Team, 2008, *R: A language and environment for statistical computing*. Available online with updates at: <http://www.cran.r-project.org>. R Foundation for Statistical Computing, Vienna, Austria. (verified 6 January 2014).

[17] Raad A.T., and R. Protz, 1971, A new method for the identification of sediment stratification in soils of the Blue Springs basin. *Geoderma* 6:23-41.

[18] Salinity Laboratory Staff, 1954, *Diagnosis and improvement of saline and alkali soils*. Agric. Handb. 60. U.S. Gov. Print. Office, Washington, DC.

[19] Schaetzl R., 1998, Lithologic discontinuities in some soils on drumlins: Theory, detection, and application. *Soil Sci.* 163(7):570-590.

- [20] Schoeneberger P.J., D.A. Wysocki, E.C. Benham, and W.D. Broderson (ed.), 2002, Field book for describing and sampling soils, Version 2.0. USDA-NRCS, National Soil Survey Center, Lincoln, NE.
- [21] Sharma A., D.C. Weindorf, T. Man, A. Aldabaa, and S. Chakraborty, 2014, Characterizing soils via portable x-ray fluorescence spectrometer: 3. Soil reaction (pH). *Geoderma* 232-234:141-147. doi: <http://dx.doi.org/10.1016/j.geoderma.2014.05.005>.
- [22] Sharma A., D.C. Weindorf, D.D. Wang, and S. Chakraborty, 2015, Characterizing soils via portable x-ray fluorescence spectrometer: 4. Cation exchange capacity (CEC). *Geoderma* 239-240:130-134 doi: <http://dx.doi.org/10.1016/j.geoderma.2014.10.001>.
- [23] Soil Science Society of America, 2014, Glossary of soil science terms. Available at <https://www.soils.org/publications/soils-glossary> (verified 18 June 2014).
- [24] Soil Survey Staff, 2004, Soil survey laboratory methods manual. USDA-NRCS. U.S. Gov. Print. Off., Washington, DC.
- [25] Soil Survey Staff, 2010, Keys to Soil Taxonomy, 11<sup>th</sup> Ed. USDA-NRCS. Lincoln, NE.
- [26] Soil Survey Staff, 2014, Kellogg soil survey laboratory methods manual; Soil survey investigations report No. 42, Version 5.0. USDA-NRCS. National Soil Survey Center, Lincoln, NE.
- [27] Stefanovits P., 1963, The soils of Hungary. 2nd ed. (In Hungarian) Akadémiai Kiadó. Budapest.
- [28] Sudduth K.A., and J.W. Hummel, 1993, Near-infrared spectrophotometry for soil property sensing. In: DeShazer, J.A., Meyer, G.E. (ed.), Proceedings of SPIE Conference on Optics in Agriculture and Forestry, 16-17 November, 1992 Boston, MA, USA, vol. 1836. SPIE, Bellingham, WA, pp. 14-25.
- [29] Swanhart S., D.C. Weindorf, S. Chakraborty, N. Bakr, Y. Zhu, C. Nelson, K. Shook, and A. Acree, 2014, Soil salinity measurement via portable x-ray fluorescence spectrometry. *Soil Science* 179(9):417-423. doi: [10.1097/SS.0000000000000088](https://doi.org/10.1097/SS.0000000000000088).
- [30] Weindorf D.C., Y. Zhu, R. Ferrell, N. Rolong, T. Barnett, B. Allen, J. Herrero, and W. Hudnall, 2009, Evaluation of portable x-ray fluorescence for gypsum quantification in soils. *Soil Sci.* 174(10):556-562. doi: [10.1097/SS.0b013e3181bbbd0b](https://doi.org/10.1097/SS.0b013e3181bbbd0b).
- [31] Weindorf D.C., Y. Zhu, P. McDaniel, M. Valerio, L. Lynn, G. Michaelson, M. Clark, and C.L. Ping, 2012a, Characterizing soils via portable x-ray fluorescence spectrometer: 2. Spodic and Albic horizons. *Geoderma* 189-190:268-277. doi: [10.1016/j.geoderma.2012.06.034](https://doi.org/10.1016/j.geoderma.2012.06.034).
- [32] Weindorf D.C., Y. Zhu, S. Chakraborty, N. Bakr, and B. Huang, 2012b, Use of portable x-ray fluorescence spectrometry for environmental quality assessment of peri-urban agriculture. *Env. Mon. Assess.* 184:217-227. doi: [10.1007/s10661-011-1961-6](https://doi.org/10.1007/s10661-011-1961-6).
- [33] Weindorf D.C., Y. Zhu, B. Haggard, J. Lofton, S. Chakraborty, N. Bakr, W. Zhang, W.C. Weindorf, and M. Legoria, 2012c, Enhanced pedon horizonation using portable x-ray fluorescence spectroscopy. *Soil Sci. Soc. Am. J.* 76(2):522-531. doi: [10.2136/sssaj2011.0174](https://doi.org/10.2136/sssaj2011.0174).
- [34] Weindorf D.C., J. Herrero, C. Castañeda, N. Bakr, and S. Swanhart, 2013a, Direct soil gypsum quantification via portable x-ray fluorescence spectrometry. *Soil Sci. Soc. Am. J.* 77:2071-2077.
- [35] Weindorf D.C., L. Paulette, and T. Man, 2013b, In-situ assessment of metal contamination via portable x-ray fluorescence spectroscopy: Zlatna, Romania. *Environmental Pollution* 182:92-100. doi: [10.1016/j.envpol.2013.07.008](https://doi.org/10.1016/j.envpol.2013.07.008).
- [36] Weindorf D.C., N. Bakr, and Y. Zhu, 2014, Advances in portable x-Ray fluorescence (PXRF) for environmental, pedological, and agronomic applications. *Advances in Agronomy* 128:1-45. doi: <http://dx.doi.org/10.1016/B978-0-12-802139-2.00001-9>.
- [37] Weindorf D.C., S. Chakraborty, A. Aldabaa, L. Paulette, G. Corti, S. Cocco, E. Michéli, D. Wang, B. Li, T. Man, A. Sharma, and T. Person, 2015, Lithologic discontinuity identification via proximal sensors. *Soil Sci. Soc. Am. J.* (Under peer review 4.22.15).
- [38] Zhu Y., D.C. Weindorf, S. Chakraborty, B. Haggard, S. Johnson, and N. Bakr, 2010, Characterizing surface soil water with field portable diffuse reflectance spectroscopy. *J. of Hydrol.* 391:133-140 doi: [10.1016/j.jhydrol.2010.07.014](https://doi.org/10.1016/j.jhydrol.2010.07.014).
- [39] Zhu Y., D.C. Weindorf, and W. Zhang, 2011, Characterizing soils using a portable x-ray fluorescence spectrometer: 1. Soil texture. *Geoderma* 167-168:167-177. doi: [10.1016/j.geoderma.2011.08.010](https://doi.org/10.1016/j.geoderma.2011.08.010).